Cancer Chemother Pharmacol (1997) 41: 61–68

ORIGINAL ARTICLE

Elizabeth S. Woo · Anne Monks · Simon C. Watkins
Angela S. Wang · John S. Lazo

Diversity of metallothionein content and subcellular localization in the National Cancer Institute tumor panel

Received: 22 November 1996 / Accepted: 3 April 1997

Abstract Metallothioneins (MTs) are major thiol-containing intracellular proteins that bind metals, are induced by stress, and have been implicated in resistance to drugs and heavy metals. *Purpose*: To examine the hypothesis that the protective functionality of MT may be dictated by its subcellular localization. *Methods*: We analyzed the basal MT content in 53 adherent cell lines of the National Cancer Institute (NCI) tumor panel and quantified the nuclear/cytoplasmic distribution of MT using confocal laser scanning microscopy and a recently described immunofluorescence-based algorithm. *Results*: Among these cell types we found a 400-fold range in the basal MT levels and a tenfold range in the ratio of the nuclear to cytoplasmic MT immunostaining that was independent of basal MT content. Total MT levels and nuclear/cytoplasmic distribution were independent of total glutathione content, suggesting autonomous regulation of these protective protein and nonprotein thiol pools. Approximately 50% (29/53) of the cell lines had a greater nuclear than cytoplasmic MT density and were defined as having a karyophilic phenotype. Tissue specificity of MT localization was seen with breast cancer cell lines, which were cytoplasmophilic, whereas prostate-derived cells were karyophilic. Among the 25 000 unrestricted compounds in the NCI database, we detected a correlation between total basal MT levels and resistance to $CdCl_2$, four Pt- and two Cu-containing compounds. High nuclear/cytoplasmic MT values correlated with resistance to six Cu-, six Pb-, and one Zn-containing compounds. *Conclusions*: These results demonstrated significant diversity in MT content and subcellular localization in human tumor cells. Moreover, both basal MT levels and subcellular distribution appeared to be determinants of cellular responsiveness to metal-containing compounds.

Key words Tumor cells · Immunofluorescence · Chemotherapy · Metals

Supported by NIH grants CA61299 (J.S.L.) and CA62781 (E.S.W.)

E.S. Woo · A.S. Wang · J.S. Lazo (✉)
Department of Pharmacology, School of Medicine,
University of Pittsburgh, Pittsburgh, Pennsylvania 15261, USA
Tel. (412)648-9319, Fax (412)648-2229; E-mail: lazo@pop.pitt. edu

S.C. Watkins
Department of Cell Biology and Physiology,
School of Medicine, University of Pittsburgh, Pittsburgh,
Pennsylvania 15261, USA

J.S. Lazo
Experimental Therapeutics Program,
University of Pittsburgh Cancer Institute,
University of Pittsburgh, Pittsburgh,
Pennsylvania 15261, USA

A. Monks
SAIC Frederick, NCI-FCRDC,
Frederick, MD 21701, USA

Introduction

Because of the high cysteine content in metallothioneins (MTs), these low molecular weight proteins bind heavy metals and can protect cells against the toxicity of metals such as cadmium. Previous studies have also implicated MT in resistance to some anticancer drugs and mutagens [18]. In addition, MT can protect cells against nitrogen-based reactive species or oxygen-based radicals, such as those generated by cytokines (e.g. tumor necrosis factor α) or chemicals (e.g. *tert*-butyl hydroperoxide) [20, 29, 30]. MT can be induced in isolated cells and in intact animals by a host of stimuli, including heavy metals, cytokines, alterations in oxygen tension, oxidants, UV irradiation, hormones, and some drugs [3, 18]. Most of the studies showing a role for MT in protecting cells or tissues have exploited the inducibility of MT. There is considerably less information about the relative importance of basal or uninduced MT in protecting cells or

tissues. That basal MT may help determine cellular sensitivity to some toxic substances has recently been suggested with animals and cells lacking MT due to gene deletion; they are more susceptible to the toxicity of cadmium [16, 21, 22].

MT has been found in both the cytoplasm and nucleus of normal and malignant cells. The mechanism and biological significance of its subcellular localization has largely been ignored. Some have suggested that nuclear localization is related to the cellular content of MT [2] or cell cycle phase [32]. Recent observations in our laboratory have indicated an energy-dependent subcellular retention system for MT that is cell type specific [33].

The National Cancer Institute (NCI) has established a panel of human tumor cell lines to evaluate potential antineoplastic agents, some of which have heavy metal components [23, 27]. These cells are cultured under uniform conditions and provide a unique opportunity to perform comprehensive studies with cells grown at a single site. We examined these cell lines for variability in basal MT content and subcellular distribution. Because MT can bind to the major nonprotein thiol, glutathione (GSH) [6], we also used this cellular library to investigate the relationship between basal GSH levels and either basal MT levels or subcellular localization. Finally, the basal MT phenotype was examined for correlation to cellular responsiveness to more than 25 000 agents under investigation for antineoplastic activity.

Materials and methods

Cell culture and reagents

We limited our analysis to the 53 adherent human cell lines in the NCI tumor cell line panel to maintain consistency in culturing, fixing, staining, and mounting protocols. All cells were maintained and cultured in a humidified atmosphere containing 5% CO_2 at 37 °C and have been previously described [23]. Cytotoxicity data were obtained from the NCI database. All reagents used in our studies were obtained from Sigma (St. Louis, Mo.), unless indicated otherwise.

MT quantitation

Total cellular MT was quantified by the cadmium-binding assay, as reported previously [29]. Briefly, subconfluent cells were removed from the monolayer with a trypsin solution and lysed in 10 m*M* Tris buffer, pH 7.4, containing 1 μg/ml $CdCl_2$ by three successive freeze–thaw cycles and sonication. Total MT was determined by quantifying the binding of carrier-free $^{109}CdCl_2$ (specific activity, 1 mCi/μg Cd; Amersham, Arlington Heights, Ill.) to the low molecular weight fraction of cleared cellular lysates, and normalizing to total protein content. Only cadmium-binding data falling within the linearity range of the assay, as determined by standard curves of rabbit liver MT (Sigma) were statistically analyzed. The results represent triplicate samples analyzed in three to six independent experiments.

Immunolocalization of MT

Cell fixing and permeabilization protocols were as described previously [14]. Cells were incubated at room temperature for 1–2 h with approximately 5 μg/ml (specific IgG concentration) of either preimmune rabbit serum or carboxymethylindocyanine CY3.18-conjugated affinity-purified rabbit antiserum (M2p-Cy3), which recognizes the two major human MT isoforms: MT I and MT II [17, 33]. Following three successive washes, slides were mounted and examined on a Nikon FX-A fluorescence microscope at 60 × magnification. Constant emission intensity of the mercury arc lamp, the illumination source for the microscope, was maintained by replacing bulbs every 120 h, daily alignment to ensure centration of illumination, and adequate warm-up time to achieve stable output. The absorption and emission maxima for Cy3.18 are 554 nm and 568 nm, respectively. No reactivity was observed with preimmune rabbit serum or in the presence of excess MT.

Nuclei were delineated by staining fixed cells with 2 μg/ml Hoechst 33342 (Molecular Probes, Eugene, Ore.) for 10 min at room temperature. Quantification of the nuclear/cytoplasmic (N/C) distribution was performed using the Optimas image acquisition and analysis program as previously described [33]. For each field of cells, single unit values for nuclear and cytoplasmic MT mean labeling intensity were derived. The mathematical means from three fields of cells (10–200 cells/field) were calculated; thus, the N/C ratios represent data from 30 to 600 cells/cell line. To minimize experimental variability, slides were prepared on the same day, stored at 4 °C in light-protected trays, and analyzed in three batches within 48 h. As an internal control, replicate samples from four cell lines (SNB-75, TK10, SNB-19, and OVCAR-3) were randomly inserted for microscopic and algorithmic analysis. In all cases both quantitative and qualitative similarities were observed.

Statistical analyses of MT content N/C location and drug responsiveness

COMPARE, a pattern recognition program [1, 10, 19, 27], was used to determine correlations between MT content in the cancer cell lines and chemosensitivity/resistance data from approximately 25 000 unrestricted compounds comprising the NCI database of investigative antineoplastic drugs. Following the previously described convention of the COMPARE program, [1, 10, 19], a "mean graph" for MT content was constructed by calculating a grand mean of MT content from the individual means of 53 cell lines in the NCI tumor cell panel, which was then used to compare each cell line mean with the grand mean[1]. The MT mean graph was compared with analogously formatted mean graphs for other agents, based on mean GI50 (growth inhibitory concentration in 50% of cells) values of each agent in the NCI data base, where higher levels of MT were assumed to be associated with resistance. COMPARE ranked by Pearson correlation coefficients the compounds most closely associated with the MT profile. Correlations of MT N/C distribution with drug resistance/sensitivity were obtained in a similar manner by calculating the grand mean of N/C ratios and generating an N/C mean graph. Here, the COMPARE analysis was conducted in two ways: (1) association of the karyophilic phenotype (high N/C) with resistance, and (2) association of the cytoplasmophilic phenotype (low N/C) with resistance. Enrichment of metals in the 100 top correlates was assessed with an Exact binomial test.

Results

Intracellular MT content and distribution

Total basal intracellular MT content in 53 adherent cell lines of the NCI tumor cell panel spanned a 400-fold

[1] Additional information about the NSC assignments and the COMPARE Program can be found on the World Wide Web site of http://epnsw1.ncifcrf.gov:2345/dis3d/dtp.html

range (Table 1), from 0.009 μg MT/mg protein (SKOV-3) to 3.839 μg MT/mg protein (LOX IMVI). The median value was 0.128 ± 0.017 μg MT/mg protein. To facilitate analyses with the NCI database, we generated a MT mean graph (Figure 1A) by subtracting the mean basal MT content of all cell lines (grand mean = 0.354 μg/mg protein) from the basal MT level of individual cell lines. Figure 1A is also a visual presentation of the MT content according to tumor types. Bars to the left of the center line (grand mean) indicate cell lines with lower MT levels than the grand mean; bars to the right indicate cells with higher MT levels. Interestingly, the mean MT levels for all of the ovarian- and breast-derived cells were lower than the mean (0.04 and 0.14 μg/mg protein, respectively) in contrast to the mean values for renal and melanoma cancer cell lines, which were greater than the grand mean at 0.735 and 0.767 μg/mg protein, respectively. The doxorubicin-resistant breast

Table 1 MT content, N/C ratio, and histological tumor type of cancer cell lines. MT levels were determined by the cadmium binding assay and reflect mean values from three to six independent experiments. N/C ratios were computed from immunofluorescence images of cells stained with M2p-CY3. Mean values are from 30–600 cells/cell line. Standard errors are included for all mean determinations (*nd* not determined)

Cell line	Tumor type	[MT] (μg/mg protein)		N/C ratio	
		Mean	SEM	Mean	SEM
SK-OV-3	Ovary	0.009	0.001	0.68	0.130
NCI-H522	Lung	0.012	0.002	1.52	0.169
NCI-H322M	Lung	0.013	0.002	0.74	0.220
HCC-2998	Colon	0.022	0.008	3.24	0.978
A498	Renal	0.023	0.001	1.47	0.139
OVCAR-3	Ovary	0.023	0.003	0.93	0.140
OVCAR-5	Ovary	0.024	0.004	1.07	0.223
HOP-62	Lung	0.025	0.005	1.22	0.197
U251	CNS	0.030	0.006	1.20	0.152
OVCAR-4	Ovary	0.030	0.010	1.44	0.254
CAKI-1	Renal	0.034	0.009	1.98	0.212
MCF7	Breast	0.036	0.001	0.55	0.034
IGROV-1	Ovary	0.036	0.003	nd	nd
SK-MEL-2	Melanoma	0.050	0.013	0.45	0.072
NCI-H226	Lung	0.054	0.029	3.85	1.923
SK-MEL-5	Melanoma	0.058	0.005	0.97	0.124
HT29	Colon	0.060	0.003	1.34	0.219
SNB-19	CNS	0.067	0.004	2.68	0.517
T-47D	Breast	0.075	0.007	1.00	0.050
NCI-H460	Lung	0.075	0.016	1.41	0.225
MCF7/ADR-RES	Breast	0.086	0.012	1.32	0.149
SF-268	CNS	0.106	0.007	1.28	0.034
MALME-3M	Melanoma	0.108	0.004	3.91	1.072
SN12C	Renal	0.111	0.004	0.82	0.138
DU-145	Prostate	0.117	0.013	4.00	0.100
VACC-257	Melanoma	0.119	0.027	0.88	0.058
SNB-75	CNS	0.128	0.017	0.92	0.129
OVCAR-8	Ovary	0.133	0.004	1.93	0.226
HOP-92	Lung	0.138	0.047	0.77	0.043
BT-549	Breast	0.150	0.015	0.89	0.135
MDA-MB-231	Breast	0.160	0.018	0.69	0.088
KM12	Colon	0.161	0.003	2.37	0.008
HS 578T	Breast	0.163	0.051	0.85	0.170
SW-620	Colon	0.166	0.015	0.97	0.115
RXF393	Renal	0.167	0.022	nd	nd
VACC-62	Melanoma	0.182	0.000	0.74	0.196
SF-539	CNS	0.213	0.013	0.60	0.056
COLO 205	Colon	0.218	0.009	1.80	0.276
ACHN	Renal	0.244	0.022	2.90	1.186
A549	Lung	0.253	0.005	0.91	0.271
NCI-H23	Lung	0.299	0.066	0.87	0.139
MDA-MB-435	Breast	0.311	0.010	0.92	0.078
HCT-15	Colon	0.377	0.016	1.91	0.302
TK10	Renal	0.424	0.020	2.67	0.779
PC-3	Prostate	0.442	0.013	1.88	0.693
EKVX	Lung	0.539	0.011	2.59	0.837
SK-MEL-28	Melanoma	0.578	0.004	1.57	0.471
HCT-116	Colon	1.159	0.037	0.76	0.125
M14	Melanoma	1.202	0.032	1.45	0.189
SF-295	CNS	1.404	0.106	2.77	0.922
UO-31	Renal	1.626	0.329	2.78	0.865
786-0	Renal	2.681	0.338	0.96	0.025
LOX IMVI	Melanoma	3.839	0.228	2.04	0.280

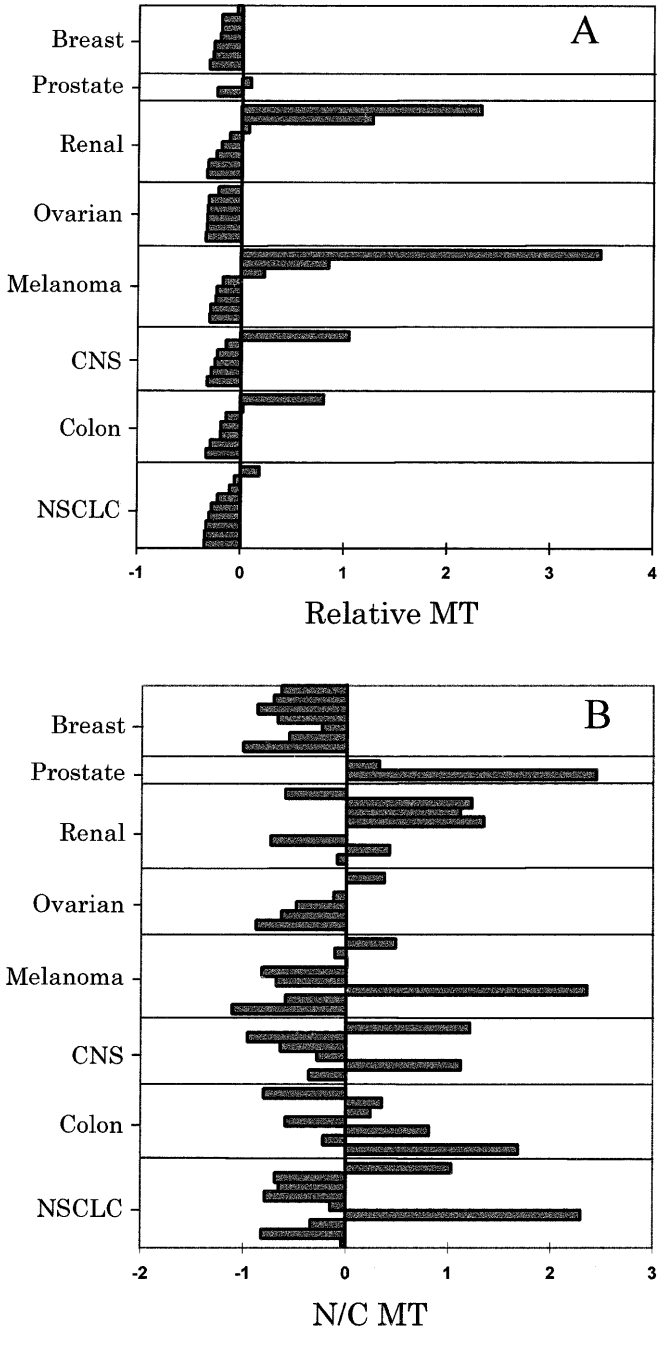

Fig. 1A,B Mean graphs of MT content and N/C ratio. Center line represents grand mean MT level **(A)** or N/C ratio **(B)** for NCI cell panel. Each bar represents data from a cell line and they are identically ordered for each profile according to histological tumor type. In ascending order: *non-small-cell lung cancer tumor* (*NSCLC*) NCI-H522, NCI-H322M, HOP-62, NCI-H226, NCI-H460, HOP-92, A549, NCI-H23, EKVX; *colon* HCC-2998, HT29, KM-12, SW-620, COLO 205, HCT-15, NCT-116; *CNS* U251, SNB-19, SF-268, SNB-75, SF-539, SF-295; *melanoma* SK-MEL-2, SK-MEL-5, MALME-3M, VACC-257, VACC-62, SK-MEL-28, M14, LOX IMVI; *ovarian* SK-OV-3, OVCAR-3, OVCAR-5, OVCAR-4, OVCAR-8; *renal*, A498, CAKI-1, RXF393, TK10, UO-31, 786-O; *prostate* DU-145, PC-3; *breast* MCF-7, T-470, MCF71ADR-RES, BT-549, MDA-MB-231, HS578T, MDA-MB-435. Leftward projections of bars from the center line indicate MT levels or N/C ratios lower than their respective grand means; rightward projections reflect higher MT levels or N/C ratios

cancer cell line, MCF-7/ADR-RES, had 2.4-fold more MT than the wildtype MCF-7 cells ($P < 0.05$; Table 1).

The subcellular distribution of MT was determined by direct immunofluorescence microscopy using our previously characterized anti-MT antiserum, which recognizes the two major human isoforms: MT I and MT II [33]. Visual examination of the immunofluorescent images revealed several distinct staining patterns characterized by punctate or diffuse distribution and heterogeneous and homogeneous staining among cells. The MT distribution pattern was not unique to this antibody, as we have also observed similar staining patterns with a commercially available monoclonal antibody to MT (DAKO, Carpinteria, Calif.). To quantify the subcellular distribution patterns in human tumor cells, we examined the N/C distribution of MT using anti-MT antiserum, and counterstained cells with Hoechst 33342 to delineate nuclei. Using our newly developed algorithm [33] with the digitized fluorescent images, we analyzed between 30 and 600 cells of each cell type and confirmed significant differences in the basal MT N/C distribution. As presented in Table 1, the N/C ratios ranged from 0.45 (SK-MEL-2, highest cytoplasmic MT) to 4.00 (DU-145, highest nuclear MT) and were consistent with the visual examination of immunofluorescent images.

In Fig. 2, two representative cell types with low N/C ratios, SK-MEL-2 (Fig. 2A) and NCI-H23 (Fig. 2B), are compared with cells with high N/C ratios, namely EKVX (Fig. 2C) and DU-145 (Fig. 2D). Most cell populations were very homogeneous in N/C values and apparent MT subcellular distribution as suggested by the SEM values in Table 1, but some cell types, such as HCC-2998 and NCI-H226, had quite a high SEM and were heterogeneous with respect to the subcellular distribution of MT. Approximately half (28/53) of the cell lines had N/C values >1.0. A mean graph of N/C distribution was formulated (Fig. 1B), with bars projecting to the left or right of the grand mean (1.56) representing cell lines with less or more nuclear MT, respectively. Interestingly, all breast-derived cells, which had shown low MT levels overall (Fig. 1A), demonstrated N/C values less than the grand mean, consistent with a more cytoplasmic MT phenotype (Fig. 1B). In contrast, MT appeared to be nuclear for both prostate cell lines. For the entire tumor panel, however, the N/C MT ratio was independent of total MT content.

Drug resistance and MT content and N/C location

The NCI anticancer agent database of over 25 000 unrestricted compounds was used in comparative analyses of MT content or N/C distribution. The database comprised cytotoxicity/growth inhibition determinations (48 h, continuous exposure), as measured by the sulforhodamine-B assay, for each cell line in the tumor panel. The GI50 concentrations were used to generate mean graphs and make COMPARE correlations, as

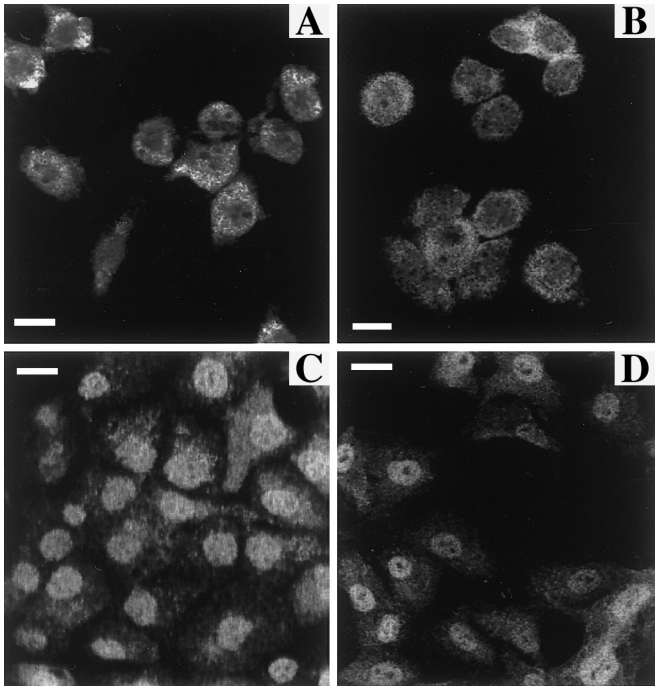

Fig. 2A–D Representative immunofluorescent images of human cells. Cells were fixed in 2% paraformaldehyde/0.1% Triton X-100 and stained with M2p-CY3. Grayscale output reflects staining intensity. **A, B** SK-MEL-2 (N/C 0.45) and NCI-H23 (N/C 0.87), respectively, which represent MT cytoplasmophilic cells. **C, D** EKVX (N/C 2.59) and DU-145 (N/C 4.00) respectively, which are MT karyophilic cells. Magnification $\times 60$ for all image acquisition; *bars* 10 μm

described by Paull et al. [27]. COMPARE cannot be used to predict absolutes, but preliminary evidence shows that when levels of a molecular target are arranged in the form of a mean graph [27] and used as a seed, then COMPARE may help identify compounds whose activity is selectively related to the expression by a cell of a given target [1, 10, 19]. Therefore, total MT content and N/C values were converted and entered as seed patterns using the "Molecular target application" of COMPARE [1, 10, 19] to search the compound database and rank compounds by Pearson correlation coefficients.

MT levels correlated with $CdCl_2$ resistance, ranking 113 out of 25 000 agents ($P < 0.05$). The 15 agents with the highest correlation with MT levels or MT N/C values are presented in Table 2. No common structural similarity was apparent among these agents, but a clear enrichment was seen for copper-containing compounds (4/15) correlated with MT N/C ($P < 0.001$). The 100 agents with the best correlation with MT levels included four platinum-containing compounds (NSC 633560, 615538, 641456, 641459) and two copper-complexes (NSC 638272, 624662), but this could have occurred by random distribution of the 1050 metal-containing compounds within the database. Interestingly, six copper (NSC 619311, 638312, 624662, 619310, 633273, 639093) and six lead complexes (NSC 173046, 628686, 628693, 628688, 628692, 628683) were among the top 100 agents correlating with N/C distribution. This was a three-fold greater enrichment of metal containing compounds than would be expected and was significantly greater than predicted by random distribution ($P < 0.001$). Therefore, our results provide the conceptual foundation for the hypothesis that basal MT N/C distribution is an important determinant of resistance to metal-containing compounds. Results using the standard agent database and COMPARE indicated that patterns of resistance for cisplatin, alkylating agents, such as melphalan and adriamycin were not associated with basal MT levels or N/C distribution.

Table 2 Top 15 drug correlates to MT content or N/C ratio.Results from COMPARE analysis were rank ordered by Pearson correlation coefficient. Resistance to the listed drugs showed the highest correlation with MT content or MT N/C ratio (*PCC* Pearson correlation coefficient)

Total MT content			MT N/C ratio		
NSC	Name/formula	PCC	NSC	Name/formula	PCC
259968	Bouvardin	0.482	656177	7-epi-10-deacetyltaxol	0.571
651849	$C_{42}H_{53}N_7O_{13}$	0.422	618533	$C_{22}H_{17}FO$	0.557
601422	Quinocarcinomycin monocitrate	0.411	173046	Diphenyllead diacetate	0.556
625129	$C_{17}H_{22}Br_2N_2$	0.402	647753	$C_{47}H_{50}ClNO_{14}$	0.518
165563	Bruceantin	0.384	627278	Thuriferic acid	0.504
625456	$C_{28}H_{54}N_2Br$	0.374	669946	$C_{21}H_{22}ClN_3O_2S_2$	0.498
643170	Ethyl 3,4-dimethoxy -α-benzoylcinnamate	0.365	628686	$C_{26}H_{22}N_2O_4Pb$	0.491
658856	$C_{19}H_{14}N_2O_2$	0.360	629014	$C_{25}H_{20}ClN_3O$	0.490
677599	$C_{43}H_{54}N_8O_{12}$	0.354	619311	$C_{14}H_{24}CuN_2S_4$	0.490
683039	Immunotoxin e23(dsFv)-PE38	0.349	638312	$C_{14}H_{13}CuN_3O_4$	0.488
637595	$C_{27}H_{18}F_6N_4O_4$	0.345	624662	$C_{36}H_{38}CuN_8O_{10}S_2$	0.486
630883	$C_{23}H_{17}N_3O_3$	0.333	650012	$C_{17}H_{14}BrClN_2O_3$	0.481
658863	$C_{15}H_{14}N_2O_2$	0.327	619310	$C_{14}H_{24}CuN_2S_4$	0.481
621102	$C_{23}H_{15}N_3O_5$	0.323	653564	$C_{16}H_{19}N_4O_5P$	0.472
668871	$C_{48}H_{53}C_{15}N_4O_{10}$	0.323	624053	$C_{16}H_{14}N_2OS$	0.468

Because MT can bind to GSH [6], basal nonprotein thiol levels may be coordinately regulated by MT. Thus, we also compared total basal MT levels with total basal GSH levels (reduced and oxidized) previously determined for these cells. We found no statistically significant correlation ($P < 0.05$).

Discussion

Our results indicate considerable diversity in the basal MT content of malignant human cells. We detected a 400-fold range in basal MT content in 53 cell lines even when cultured under similar conditions. This difference exceeds the general inducibility of MT we [14] and others [3, 11 18] have noted in individual cell types treated with agents such as interleukin-1β or glucocorticoids. Some evidence for cell type specificity in basal level and isotype patterns of MT expression has been reported [12]. The NCI tumor panel appears to retain at least some cell type specificity in basal MT expression. Interestingly, previous immunohistochemical studies [12] indicate that only 26% of all breast cancer tumors have more than 50% of cells positive for basal MT expression and this was one of the tumor types that had lower than average basal MT levels in our study. Basal MT expression appears to be subject to *cis* regulation by locus control regions, DNA methylation and basal regulatory elements in the 5′ flanking region [11, 26]. In addition DNA methylation also suppresses the basal expression of MT [11]. The kinetics and magnitude of MT inducibility, as well as inducer sensitivity, appear to be cell-type dependent [12]. In this initial study, however, we focused exclusively on basal MT and we have not yet examined the inducer sensitivity or the kinetics and magnitude of MT induction in the tumor panel.

In addition to the considerable variability in basal MT content, we also found a tenfold difference in the N/C distribution of MT among the cells studied, which was unrelated to total MT content. Because MT is a small protein (6–7 kDa) and lacks an obvious nuclear localizing sequence, passive processes should dictate its movement across the nuclear envelope. Discrete nuclear MT residence, however, has been observed in cells associated with developmental factors [25], cellular proliferation [32], and cell cycle phase [24]. Nonetheless, we have been unable to associate nuclear localization to cell cycle phases [33]. The NCI tumor panel was almost evenly divided with respect to karyophilic and cytoplasmophilic phenotypes. The factors controlling MT subcellular residence as well as the functional significance of this partitioning are not yet defined, but the NCI tumor panel could be a valuable tool to explore this topic as more biochemical information about the cells becomes available.

MT movement against a concentration gradient implies active sequestration properties, which could be explained by nuclear or cytoplasmic retention mechanisms. Recent observations from our laboratory demonstrate that nuclear sequestration of MT can be disrupted under energy-depleting conditions, suggesting the involvement of an active binding component in basal MT distribution [33]. Cellular proteins, matrices, or organelles are possible candidates; however, no such tethers have been identified for MT thus far. Brouwer et al. [6] have reported the formation of complexes between GSH and Cd/Zn-speciated MT I and MT II from rabbit liver in vitro. Furthermore, MT synthesis may regulate sulfur metabolism and influence the synthesis and, thus, the levels of nonprotein thiols such as GSH [11]. In our studies, GSH content showed neither direct nor inverse correlation with MT levels, suggesting independent regulation of the major cellular thiol sources. Like MT, the intracellular distribution of GSH is thought to be dictated by passive processes, yet subcellular pools of GSH have been observed [5, 31]. Depletion of the nuclear pools of GSH with buthionine sulfoximine appears to sensitize ovarian adenocarcinoma cells to the anticancer drug, melphalan [5]. Thus, we cannot exclude the possibility that colocalization of GSH and MT in the proper subcellular compartment may confer biological function. The development of new cytometry methods [31] should assist in evaluating that question with the NCI tumor panel.

The most widely accepted biological role for MT is to protect cells and tissues against heavy metals, most notably cadmium [3, 11]. Nonetheless, MT I transgenic mice are not protected against cadmium-induced toxicity during pregnancy or cadmium-induced lethality [8]. Moreover, resistance to cadmium in human tumors can be caused by altered cadmium uptake or expression of the autosomal recessive *cdm* gene [8, 9]. Consequently, we used the pattern recognition program, COMPARE, to examine the hypothesis that basal MT may be responsible for resistance to heavy metals. This database was also interesting because previous studies have suggested that MT could protect cells against alkylating agents, cisplatin, oxidants, and cytokines [16, 18, 29]. Although the COMPARE pattern recognition program always produces a list of compounds and correlations, it also provides an unbiased method to identify compounds associated with a specific phenotype. Thus, *mdr1* expression [1] and rhodamine efflux patterns [19] have been used as seed patterns in COMPARE analyses to identify previously unknown substrates for P-glycoprotein. Query of the NCI database for correlation to DT-diaphorase activity not only revealed sensitivity to the prototypic bioreductive agent, mitomycin C, but also an investigational drug, EO9 [10].

MT binds and inactivates $CdCl_2$. It is, therefore, noteworthy that resistance to $CdCl_2$ was among the highest correlates (113 out of 25 000 agents) with high basal MT levels, indicating that basal MT is an important factor in determining sensitivity to this heavy metal despite other potential mechanisms of resistance. The top 100 correlates to basal MT levels, however, showed no significant enrichment of metal-containing compounds, suggesting that either MT subcellular distribution or

other cellular factors are important for resistance. Unfortunately, the mechanisms of action for many compounds identified in the high correlate population are not currently known, making it difficult to deduce the possible theoretical basis for the correlation. Curiously, we found basal MT levels correlated most highly with resistance to bouvardin and bruceantin, both of which are antitumor antibiotics that bind eukaryotic ribosomes and are thought to function by inhibiting protein synthesis [4, 28]. Perhaps this is related to previously characterized requirements for zinc in protein synthesis and mRNA expression [13] and the importance of MT in zinc homeostasis [11]. It is notable that cisplatin, melphalan, chlorambucil, and doxorubicin are absent from the high correlate population in both standard agent and total agent databases because some but not all previous studies [18] suggest either direct or indirect mechanisms involving MT in cytoprotection against these agents.

There has been some speculation that MT N/C location may be linked to a particular function. Apometallothionein can extract zinc from zinc finger proteins, such as Sp1, and block their ability to bind DNA and activate transcription [34]. Chubatsu and Meneghini [7] found that V79 cells are protected against H_2O_2-induced DNA strand breaks when MT is located in the nucleus. Cytoprotection from both oxygen and nitrogen-based radicals is afforded in NIH3T3 cells by cytoplasmic MT [29, 30]. In a study with several prostate cell lines, we have found that nuclear MT is more efficient at protecting against cisplatin cytotoxicity [15]. In the present study with 53 cell lines, the COMPARE correlation between N/C distribution and 25 000 compounds resulted in 13 metal-containing compounds (six copper, six lead, one zinc) in the top 100 correlations (13%) representing three times the number one would expect in a random distribution of metals (4.2%) in these 100 compounds. Of the top 15 compounds, four contained copper. These results support a potential causative relationship between N/C localization and resistance to some metal-containing compounds and are consistent with a role of nuclear MT in protecting cells against heavy metals. Interestingly, neither high nor low N/C ratio correlated with resistance to $CdCl_2$, which may reflect the need for MT to be in both cytoplasmic and nuclear compartments for protection. We also found no evidence for a correlation between resistance to cisplatin, doxorubicin, chlorambucil or melphalan and a high N/C ratio. There are two potential explanations for the failure to detect a relationship between MT levels or distribution and these anticancer drugs. First, the conventional cytotoxicity assay used by the NCI requires continuous exposure to the agent for 48 h, which is well within the time required for MT induction. Thus, the kinetics and magnitude of MT induction could be more important than the basal MT levels, which is what was measured in this initial study. Such a hypothesis could be tested with a limited number of compounds. Alternatively, other factors may have a more dominant position in the hierarchy of drug resistance. It is clear that a multitude of factors affect cell sensitivity to cisplatin, melphalan, chlorambucil, doxorubicin and oxidants, including differences in drug uptake and retention, sequestration, DNA repair mechanisms, antioxidants, cellular redox status, modulation of cellular responses by Bcl-2 or Bax, and cell cycle kinetics by p^{53} or p^{21}.

In conclusion, we have established that considerable diversity in MT content and subcellular localization exists among cell lines grown under similar conditions but derived from different histological tumor types. Cellular resistance to metals, such as $CdCl_2$, correlates with basal levels of MT in the cell lines. Our results support a functional role for MT located in discrete cellular compartments. The availability of these results with the NCI database may be useful in elucidating unique biological roles for MT, as well as providing insight into anticancer drug mechanisms.

References

1. Alvarez M, Paull K, Monks A, Hose C, Lee JS, Weinstein J, Grever M, Bates S, Fojo T (1995) Generation of a drug resistance profile by quantification of mdr-1-P-glycoprotein in the cell lines of the National Cancer Institute anticancer drug screen. J Clin Invest 95: 2205
2. Banerjee D, Onosaka S, Cherian MG (1982) Immunohistochemical localization of metallothionein in cell nucleus and cytoplasm of rat liver and kidney. Toxicology 24: 95
3. Bauman JW, Liu J, Liu YP, Klaassen CD (1991) Increase in metallothionein produced by chemicals that induce oxidative stress. Toxicol Appl Pharmacol 110: 347
4. Boger DL, Patane MA, Jin Q, Kitos PA (1994) Design, synthesis and evaluation of bouvardin, deoxybouvardin and RA-I-XIV pharmacophore analogs. Bioorg Med Chem 2: 85
5. Britten RA, Green JA, Broughton C, Browning PG, White R, Warenius HM (1991) The relationship between nuclear glutathione levels and resistance to melphalan in human ovarian tumour cells. Biochem Pharmacol 41: 647
6. Brouwer M, Hoexum-Brouwer T, Cashon RE (1993) A putative glutathione-binding site in CdZn-metallothionein identified by equilibrium binding and molecular-modeling studies. J Biochem 294: 219
7. Chubatsu LS, Meneghini R (1993) Metallothionein protects DNA from oxidative damage. J Biochem 291: 193
8. Dalton T, Fu K, Enders GC, Palmiter RD, Andrews GK (1996) Analysis of the effects of overexpression of metallothionein-I in transgenic mice on the reproductive toxicology of cadmium. Environ Health Perspect 104: 68
9. Enger MD, Tesmer JG, Travis GL, Barham SS (1986) Clonal variation of cadmium response in human tumor cell lines. Am J Physiol 250: C256
10. Fitzsimmons SA, Workman P, Grever M, Paull K, Camalier R, Lewis AD (1996) Reductase enzyme expression across the National Cancer Institute tumor cell line panel: correlation with sensitivity to mitomycin C and E09. J Natl Cancer Inst 88: 259
11. Hamer DH (1986) Metallothionein. Annu Rev Biochem 55: 913
12. Jahroudi N, Foster R, Price-Haughey J, Beitel G, Gedamu L (1990) Cell-type specific and differential regulation of the human metallothionein genes. J Biol Chem 265: 6506
13. Kimball SR, Chen SJ, Risica R, Jefferson LS, Leure-duPree AE (1995) Effects of zinc deficiency on protein synthesis and expression of specific mRNAs in rat liver. Met Clin Exp 44: 126
14. Kondo Y, Kuo S-M, Lazo JS (1994) Interleukin β mediated metallothionein induction and cytoprotection against cadmium

and *cis*-diamminedichloroplatinum. J Pharmacol Exp Ther 270: 1313
15. Kondo Y, Kuo S-M, Watkins SC, Lazo JS (1995) Metallothionein localization and cisplatin resistance in human hormone-independent prostatic tumor cell lines. Cancer Res 55: 474
16. Kondo Y, Woo E, Michalska AE, Choo AC, Lazo JS (1995) Metallothionein null cells have increased sensitivity to anticancer drugs. Cancer Res 55: 2021
17. Kuo S-M, Kondo Y, DeFilippo JM, Ernstoff MS, Bahnson RR, Lazo JS (1994) Subcellular localization of metallothionein IIA in human bladder tumor cells using a novel epitope-specific antiserum. Toxicol Appl Pharmacol 125: 104
18. Lazo JS, Pitt BR (1995) Metallothioneins and cell death by anticancer drugs. In: Cho AK, Blaschke TF, Loh HH, Way JL (eds) Annual review of pharmacology and toxicology. Annual Reviews, Palo Alto, pp 635
19. Lee JS, Paull K, Alvarez M, Hose C, Monks A, Grever M, Fojo AT, Bates S (1994) Rhodamine efflux patterns predict P-glycoprotein substrates in the National Cancer Institute drug screen. Mol Pharmacol 46: 627
20. Leyshon-Sorland K, Morkrid L, Rugstrad HE (1993) Metallothionein: a protein conferring resistance in vitro to tumor necrosis factor. Cancer Res 53: 4874
21. Masters BA, Kelly EJ, Quaife CJ, Brinster RL, Palmiter RD (1993) Targeted disruption of metallothionein I and II genes increases sensitivity to cadmium. Proc Natl Acad Sci USA 91: 584
22. Michalska AE, Choo KHA (1993) Targeting and germ-line transmission of a null mutation at the metallothionein I and II loci in mouse. Proc Natl Acad Sci USA 90: 8088
23. Monks A, Scudiero D, Skehan P, Shoemaker R, Paull K, Vistica D, Hose C, Langley J, Cronise P, Vaigro-Wolff A (1991) Feasibility of a high-flux anticancer drug screen using a diverse panel of cultured human tumor cell lines. J Natl Cancer Inst 83: 757
24. Nagel WW, Vallee BL (1995) Cell cycle regulation of metallothionein in human colonic cancer cells. Proc Natl Acad Sci USA 92: 579
25. Nartey NO, Banerjee D, Cherian MG (1987) Immunochemical localization of metallothionein in cell nucleus and cytoplasm of fetal human liver and kidney and its changes during development. Pathology 19: 233
26. Palmiter RD, Sandgren EP, Koeller DM, Brinster RL (1993) Distal regulatory elements from the mouse metallothionein locus stimulate gene expression in transgenic mice. Mol Cell Biol 13: 5266
27. Paull KD, Shoemaker RH, Hodes L, Monks A, Scudiero DA, Rubenstein K, Plowman J, Boyd MR (1989) Display and analysis of patterns of differential activity of drugs against human tumor cell lines: development of mean graph and COMPARE algorithm. J Natl Cancer Inst 81: 1088
28. Rodriguez-Fonseca C, Amils R, Garrett RA (1995) Fine structure of the peptidyl transferase centre on 23 S-like rRNAs deduced from chemical probing of antibiotic-ribosome complexes. J Mol Biol 247: 224
29. Schwarz MA, Lazo JS, Yalowich JC, Reynolds I, Kagan VE, Tyurin V, Kim T-M, Watkins SC, Pitt BR (1994) Cytoplasmic metallothionein overexpression protects NIH 3T3 cells from tert-butyl hydroperoxide toxicity. J Biol Chem 269: 15238
30. Schwarz MA, Lazo JS, Yalowich JC, Allen WP, Whitmore M, Bergonia HA, Tzeng E, Billiar TR, Robbins PD, Lancaster JR Jr, Pitt BR (1995) Metallothionein protects against the cytotoxic and DNA damaging effects of nitric oxide. Proc Natl Acad Sci USA 92: 4452
31. Thomas M, Nicklee T, Hedley DW (1995) Differential effects of depleting agents on cytoplasmic and nuclear non-protein sulphydryls: a fluorescence image cytometry study. Br J Cancer 72: 45
32. Tsujikawa K, Imai T, Kakutani M, Kayamori Y, Mimura T, Otaki N, Kimura M, Fukuyama R, Shimizu N (1991) Localization of metallothionein in nuclei of growing primary cultured adult rat hepatocytes. FEBS Lett 283: 239
33. Woo ES, Kondo Y, Watkins SC, Hoyt DG, Lazo JS (1996) Nucleophilic distribution of metallothionein in human tumor cells. Exp Cell Res 224: 365
34. Zeng J, Vallee BL, Kaji JHR (1991) Zinc transfer from transcription factor IIIA fingers to thioneine clusters. Proc Natl Acad Sci USA 88: 9984